4. C. T. Pillinger and S. S. Russell, *J. Chem. Soc. Faraday Trans.* **89**, 2297 (1993).
5. S. Amari, E. Anders, A. Virag, E. Zinner, *Nature* **345**, 238 (1990).
6. G. R. Huss, I. D. Hutcheon, G. J. Wasserburg, *Astrophys. J.* **430**, L81 (1994).
7. L. R. Nittler, C. M. O. Alexander, X. Gao, R. M. Walker, E. K. Zinner, *Nature* **370**, 443 (1994).
8. D. Heymann and M. Dzeczkaniec, *Proc. Lunar Planet. Sci. Conf.* **10**, 1943 (1979).
9. D. D. Clayton, *Astrophys. J.* **340**, 613 (1989).
10. W. M. Howard, B. S. Meyer, D. D. Clayton, *Meteoritics* **27**, 404 (1992).
11. D. D. Clayton, B. S. Meyer, C. I. Sanderson, S. S. Russell, C. T. Pillinger, *Astrophys. J.* **447**, 894 (1995).
12. G. R. Huss and R. S. Lewis, *Meteoritics* **29**, 791 (1994).
13. S. S. Russell, J. W. Arden, C. T. Pillinger, *Meteoritics Planet. Sci.*, in press.
14. ———, *Science* **254**, 1188 (1991).
15. A. B. Verchovsky, S. S. Russell, C. T. Pillinger, *Lunar Planet. Sci.* **XXIV**, 1461 (1993).
16. R. S. Lewis, *ibid.* **XXV**, 793 (1994).
17. For TEM we used a Philips Biotwin instrument operated at 120 kV and a Topcon EM-002B operated at 200 kV.
18. A. V. Fisenko et al., *Geokhimiya* **N5**, 532 (1998).
19. T. L. Daulton, D. D. Eisenhour, T. J. Bernatowicz, R. S. Lewis, P. R. Buseck, *Geochim. Cosmochim. Acta* **60**, 4853 (1996).
20. I. P. Wright and C. T. Pillinger, *U.S. Geol. Bull.* **1890**, 9 (1989).
21. I. P. Wright, S. R. Boyd, I. A. Franchi, C. T. Pillinger, *J. Phys. E* **21**, 865 (1988).
22. A. B. Verchovsky, A. V. Fisenko, L. F. Semjonova, C. T. Pillinger, *Meteoritics Planet. Sci.* **32**, A131 (1997).
23. It is known from previous studies (*30*) that both the total carbon yield and the yield of carbon at pyrolysis depends on the amount of oxygen chemically adsorbed on diamond grains. This oxygen could derive from exposure to the atmosphere or from reagents used in sample preparation, and there is even a remote chance that it is extraterrestrial. Because the diamond grains are so small and therefore have high surface area, the amount of adsorbed oxygen is substantial, giving the maximum yield of carbon for the most pure diamond sample (that is, ~80%, which corresponds to ~15% of carbon yield at pyrolysis in the form of CO + CO_2). Three Efremovka samples (ED-2, ED-3, and ED-4) with similar and relatively heavy carbon isotopic composition ($\delta^{13}C \approx -26$ per mil) have similar total and pyrolysis carbon yields (Table 1) except for the total carbon yields for ED-4. The latter seems to be contaminated with a non-carbonaceous component. In contrast, sample ED-9, having substantially lighter carbon ($\delta^{13}C = -32.7$ per mil), also has considerably higher total and lower pyrolysis carbon yields. Apart from that, these data are also in agreement with ED-9 being the coarsest fraction.
24. D. A. Shelkov, A. B. Verchovsky, H. J. Milledge, C. T. Pillinger, *Chem. Geol.* **149**, 109 (1998).
25. When considering N and noble gas abundances released by stepped combustion, it is necessary to normalize the yields of these species to the overall C content of each sample. This has been done for each step of the four extractions, and the results are presented as element-to-C ratios versus proportion of total C removed (Fig. 3).
26. We cannot exclude the possibility that the primary ion energies could be modified because of ion collisions with dust particles and gas, present along with diamonds in the place where implantation has occurred, making the ion energies just enough to stop within diamond grains.
27. An implantation mechanism was suggested earlier (*3*) on the basis of the relative abundance of ^{129}Xe in Xe-HL, which does not show any excess due to ^{129}I decay (as would be expected if Xe and I were trapped during diamond growth). In addition, the abundance of ^{4}He, ^{20}Ne, and ^{36}Ar in the individual fractions (Table 1) indicates that the smaller the grain size, the higher the relative concentration of lighter noble gases (that is, the $^{4}He/^{36}Ar$ and $^{20}Ne/^{36}Ar$ ratios decrease with increasing grain size). This is clearly not compatible with preferential noble gas losses from smaller grains (as may accompany postformational heating, for instance) but is in agreement with an implantation mechanism at which small, light ions have a shorter projected range (*31*).
28. U. Ott, *Astrophys. J.* **463**, 344 (1996).
29. For implantation to have caused the C isotopic composition to have changed by 7 per mil between fine and coarse fractions (Table 1), we need to suggest a fluence of pure ^{12}C (or strongly enriched by ^{12}C) ions providing 7 atoms of ^{12}C per 1000 C atoms of diamond. Because of the difference in the diamond grain size, the effectiveness of implantation is relatively greater in the coarse grains. The maximum difference in relative concentration of implanted species observed in this study for noble gases is about a factor of 5 (see Table 1). A similar difference translated to the isotopes of C would result in the actual measured difference in $\delta^{13}C$ between fine and coarse grain size fractions at $^{12}C_{impl}/^{12}C_{diam} = 0.01$. In this case the calculated $^{12}C/^{4}He$ ratio in the ion flux would be ~10^3. Such a high ratio is predicted to exist in the O/Ne shell of a 25 $M_\odot$ supernova (*32*) where a strong enrichment by ^{12}C is also predicted. This shell also contains a substantial fraction of ^{12}C of the star. However, there would need to be a mechanism that prevented implantation of He into diamonds from other shells (for instance, O/C, He/C, and He/N) containing relatively much more He than the O/Ne shell. Applying the same sort of logic to explain N isotope variations between the grain size fractions, we are faced with a more serious problem, as variations of $\delta^{15}N$ are an order of magnitude larger than that for $\delta^{13}C$ (Table 1). Both high $^{14}N/^{4}He$ and enrichment of ^{14}N would be required at the same time, and that is not predicted in any of the supernova shells (*32*).
30. A. B. Verchovsky and C. T. Pillinger, *Meteoritics* **29**, 543 (1994).
31. K. V. Ponganis, T. Graf, K. Marti, *J. Geophys. Res.* **102**, 19335 (1997).
32. B. S. Meyer, T. A. Weaver, S. E. Woosley, *Meteoritics* **30**, 325 (1995).
33. Supported by the Particle Physics and Astronomy Research Council and by Russian Foundation of Basic Science grant 96-05-64546 (A.V.F. and L.F.S.). We thank J. Findlay and J. R. Fryer for assistance with TEM.

30 March 1998; accepted 10 July 1998

Biogeochemical Evidence for Dinoflagellate Ancestors in the Early Cambrian

J. Michael Moldowan* and Nina M. Talyzina

Dinoflagellates are single-celled organisms that reflect the ecological conditions in modern oceans and lakes. Ultrastructural data and molecular phylogeny suggest that they originated in the Neoproterozoic, yet dinoflagellate ancestors are classified only to the Middle Triassic (~240 million years ago). Examination of dinoflagellate-specific biological markers (dinosteranes and 4α-methyl-24-ethylcholestane) in concentrated microfossils with known morphology identified ancient dinoflagellate ancestors from the Early Cambrian (~520 million years ago).

Dinoflagellates are single-celled organisms, protists, that are found in most aquatic environments and form a major part of the modern plankton. Many genera are sensitive to such conditions as water salinity and nutrients, and some genera are characteristic of latitudinal oceanic temperature zones; hence, the geographic distributions of dinoflagellates can be important indicators of environmental conditions (*1*), not only for present-day environments but also for ancient ones. Fossilized dinoflagellate cysts are widespread in Mesozoic-Cenozoic sedimentary rocks (*2*). Here we examined certain morphotypes of segregated microfossils from Lower Cambrian formations for biological markers and determined that dinoflagellates originated much earlier, at least as early as the Early Cambrian.

J. M. Moldowan, Department of Geological and Environmental Sciences, Stanford University, Stanford, CA 94305-2115, USA. N. M. Talyzina, Department of Earth Sciences, Historical Geology and Paleontology, Uppsala University, Norbyvägen 22, S-75236, Sweden.

*To whom correspondence should be addressed.

Several lines of evidence have indicated that dinoflagellates originated in the Neoproterozoic (*3*). RNA molecular sequencing and examination of mitochondrial cristae of modern organisms (*4*) suggest that dinoflagellates are older than Foraminifera and Radiolaria, which have been found in Cambrian rocks.

Organic-walled, acid-resistant microfossils of uncertain biological affinities that are classified on the basis of their morphology (acritarchs) are widely distributed in sedimentary rocks from the Proterozoic and Phanerozoic. Some acritarchs resemble dinoflagellate cysts (*5, 6*), but they do not show paratabulation and they have excystments that are different from classical archeopyles of recognized Mesozoic and younger dinocysts. Many acritarch specimens have no excystment structure. However, most modern dinocysts reach sediments before germination (*7*), and some of these can fossilize without excystment structure formation. Some Ordovician acanthomorphic acritarchs have a double-wall structure (*8*) comparable with that of dinoflagellate cysts. Certain cysts of living dinoflagellates from the

Table 1. Palynomorphs as a percentage of total organic solids in fraction were estimated by microscopic analysis. Hi and Lo are the high- and low-fluorescent fractions, respectively. *N* is the number of specimens counted in palynological slides.

Palynomorph	Hi (%) (N = 256)	Lo (%) (N = 329)
Globosphaeridium	43	1
Skiagia	14	2
Lophosphaeridium	13	2
Archaeodiscina	4	21
Leiosphaeridia	6	54
Leiomarginata	1.5	0.5
Pterospermella	0.5	0
Asteridium	3	1
Cranomarginata	1.5	0.5
Comasphaeridium	3	1
Cyanobacterial filaments	0.5	4
Membrane pieces	10	13

Table 2. Sterane ratios in fractions obtained from shale samples from Estonia and Greenland and the Visingsö Beds of Sweden. Tas, *Tasmanites* fraction; Ker, kerogen; Ext, extract; Lo, low-fluorescent fraction; Hi, high-fluorescent fraction. For sterane structures see Fig. 1. Dinosterane (**1**) stereoisomers are of the form ααα20R,23R,24R (RRR) + RRS + RSS + RSR.

Estonia				Greenland	Sweden		Ratio	Sterane ratio
Ext	Lo	Hi	Tas	Ker	Ext	Ker		
0.479	0.192	0.600	0.685	0.841	0.462	0.841	A	**3**/(**3**+**4**+**5**)*
0.224	0.069	0.154	0.044	0.086	0.233	0.078	B	**4**/(**3**+**4**+**5**)*
0.297	0.739	0.245	0.271	0.073	0.305	0.082	C	**5**/(**3**+**4**+**5**)*
0.510	0.150	0.805	0.713	0.935	0.523	0.947	D	**3**/(**3**+**4**+**5**)ααα20R
0.170	0.028	0.059	0.016	0.028	0.180	0.029	E	**4**/(**3**+**4**+**5**)ααα20R
0.319	0.822	0.136	0.270	0.037	0.297	0.024	F	**5**/(**3**+**4**+**5**)ααα20R
0.051	0.000	0.035	0.000	0.005	0.051	0.080	G	**1**/(**1**+**2**+**3**+**4**+**5**)ααα20R
0.035	0.000	0.016	0.003	0.004	0.063	0.049	H	**2**/(**1**+**2**+**3**+**4**+**5**)ααα20R

*Sum of four stereoisomers for Steranes **3**, **4**, and **5** : 5α,14α,17α,20S (ααα20S) + αββ20R + αββ20S + ααα20R.

order Gymnodiniales lack clearly defined archeopyles or reflected tabulation (*9*). The relation between the dinosporin cysts *Gyrodinium*, *Cochlodinium*, and *Pheopolykriskos* and their theca have only been established by incubation experiments (*10*). In sum, the morphological evidence has not been sufficient to establish links between acritarchs and dinoflagellates.

We investigated acritarchs of the Lükati Formation, which is attributed to the Dominopol (= the Talsy) regional stage that is correlated with the Atdabanian stage of the Early Cambrian (*11*). Lükati Formation glauconite clay samples were collected in Kopli quarry, Tallinn, Estonia. The sediment was demineralized with HCL and HF to extract the acid-insoluble organic remains. The extracted kerogen contained 11 acritarch genera, 3 species of *Tasmanites*, a genus attributed to prasinopycean algae (*12*), cyanobacterial sheaths, and amorphous organic tissues. Tasmanitids were separated from the sample by water filtration through a 67-μm mesh net. A fluorescence-activated cell sorter (FACS) was used to separate the remaining organic matter into "high-fluorescent" and "low-fluorescent" fractions.

The palynomorphs were well preserved, yellow in color, and transparent and produced an autofluorescence signal. This is consistent with a thermal alteration index (TAI) of about 1, suggesting that the sediment was not heated above 50°C (*13*). The autofluorescence intensity is different in certain acritarch morphotypes (*14*). The high-fluorescent fraction contained 76% acanthomorphic acritarchs plus specimens of *Lophosphaeridium*, whereas the low-fluorescent fraction was dominated by leiosphaerids and archaeodiscins (Table 1).

We heated the fractionated acritarchs in evacuated sealed glass tubes at 310°C for 72 hours. After the kerogen was cooled to room temperature, we extracted biomarkers using filtration in methylene chloride. We analyzed the extracts for various biomarkers including steranes, hopanes, and tricyclic terpanes using metastable reaction monitoring–gas chromatography–mass spectrometry (MRM-GC-MS) (*15*). Of these compounds, steranes (Table 2) are generally of eukaryotic origin (*16*).

Dinosterane and 4α-methyl-24-ethylcholestane (compounds **1** and **2**, respectively, Fig. 1) are indicative for dinoflagellates. The dinosterane carbon structure occurs in sterols found in high concentrations in numerous modern dinoflagellate species and has rarely been found in other taxa (*17, 18*). Both dinoflagellates and haptophytes (prymnesiophytes) contain sterol precursors for 4α-methyl-24-ethylcholestane (*18, 19*); however, haptophytes have not been found to have acid-resistant organic walls and do not show morphological similarity to the segregated acritarchs (*6*). The common steranes, cholestane (C_{27}), 24-methylcholestane (C_{28}), and 24-ethylcholestane (C_{29}) (compounds **3** to **5**, respectively, Fig. 1) were found in all extracts (Table 2). The ratio of dinosterane and 4α-methyl-24-ethylcholestane to these (desmethyl)steranes (ratios G and H, Table 2) show which extracts were influenced by dinoflagellates or their close relatives. Among the kerogen pyrolysates, only the high-fluorescent fraction had abundant dinoflagellate steranes. Therefore, the dinosterane and 4α-methyl-24-ethylcholestane producers must be included from among the genera *Globosphaeridium, Skiagia*, and *Lophosphaeridium*, which are predominant (70%) in the high-fluorescent fraction (Table 1).

An extract of the whole sediment was also prepared (*20*) and analyzed for comparison. The whole-rock extract represents nonpreserved biota and contained higher relative abundances of dinosterane and 4α-methyl-24-ethylcholestane than the fossil pyrolysates. This implies that an important component of the algal community had a dinoflagellate affinity. Biomarkers are organic molecules that are stable at moderate temperatures, which can be preserved in rocks even when recognizable fossils are absent. Therefore, some of the protists with dinoflagellate affinities probably did not form a stable cyst, and their membranes were eventually degraded over 520 million years of diagenesis to liberate these biomarkers in the free lipids of the rock. This is in agreement with what is known about modern dinoflagellates, many of which do not produce fossilizable cysts (*10*).

The occurrence of dinoflagellate-related steranes was also observed in the extracts and kerogen pyrolysates of two additional samples from the Lower Cambrian Buen Formation in North Greenland and the upper Riphean Visingsö Beds (lower part) from Sweden (Table 2). *Skiagia* and *Comasphaeridium*, which are present in the Lükati Formation high-fluorescent fraction, are dominant in the Greenland sample and could be responsible for the dinosterane and 4α-methyl-24-ethylcholestane liberated from its kerogen. The kerogen analyzed from the Visingsö sample did not contain any genera discussed above, and it was not clear which particular microfossils (or whether they have been preserved) in these sediments were dinosterane producers. Our biomarker analyses support earlier

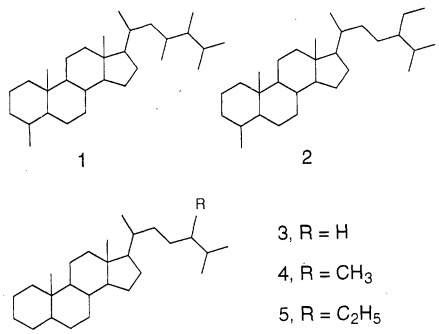

Fig. 1. Steranes analyzed in extracts and acritarchs: **1** = 4α,23,24-trimethylcholestane = dinosterane, **2** = 4α-methyl-24-ethylcholestane, **3** = cholestane, **4** = 24-methylcholestane, and **5** = 24-ethylcholestane.

reports of dinosterane occurrences in Proterozoic sediments from Bitter Springs and Pertatataka formations, central Australia (*16*), and the Nonesuch Formation in the North American mid-continent rift (*21*). The presence of dinoflagellate relatives among acritarchs explains the continuous record of dinosteroids from Precambrian to Cenozoic source rocks from numerous localities worldwide (*16, 22*).

The fossilized matter available for paleontological investigation represents less than 1% of organisms that once existed on Earth. A high abundance of related specimens in a particular age suggests that there was an earlier radiation. Various kinds of simply structured, rounded acritarchs and dinoflagellate biomarkers coexist in upper Riphean rocks, although the dinoflagellate affinity of any particular Proterozoic genus requires further investigation. Dinosterane-containing acanthomorphic acritarchs are widespread in Lower Cambrian sediments. These results suggest the evolutionary sequence in which dinoflagellate ancestry originated by the Late Riphean (~800 million years ago); specimens with processes became abundant in the Early Cambrian; and finally, the branch of dinoflagellates with classical archeopyles and paratabulation developed in the Middle Triassic.

References and Notes

1. B. Dale in *Palynology: Principles and Applications*, J. Jansonius and D. C. McGregor, Eds. (American Association of Stratigraphic Palynologists Foundation, Dallas, TX, 1996), vol. 3, pp. 1249–1277.
2. D. K. Goodman, in *The Biology of Dinoflagellates*, vol. 21 of *Botanical Monographs*, F. J. R. Taylor, Ed. (Scientific Publications, Oxford, 1987), pp. 649–722; R. Helby, R. Morgan, A. D. Partridge, in *Assoc. Australas. Palaeontol. Mem. 4* (1987), p. 1.
3. A. H. Knoll, in (*1*), vol. 1, pp. 51–81.
4. J. H. Lipps, in *Fossil Prokaryotes and Protists*, J. H. Lipps, Ed. (Blackwell, Boston, 1993), pp. 1–10.
5. L. Margulis and K. V. Schwartz, *Five Kingdoms: An Illustrated Guide to the Phyla of Life* (Freeman, San Francisco, 1982).
6. H. Tappan, *The Paleobiology of Plant Protists* (Freeman, San Francisco, 1980); C. V. Mendelson, in (*4*), pp. 77–104.
7. D. M. Anderson, J. J. Lively, E. M. Reardon, C. A. Price, *Limnol. Oceanogr.* **30**, 1000 (1985).
8. F. Martin and G. Kjellström, *Neusser Jahrb. Geol. Palaeontol. Monatsh.* **1973**, 44 (1973).
9. D. Wall and B. Dale, *Micropaleontology* **14**, 265 (1968).
10. R. A. Fensome *et al.*, *Micropaleontol. Spec. Pap. 7* (1993).
11. K. Mens, J. Bergström, K. Lendzion, *Valgus Tallin.* **1987** 14 (1987).
12. D. Guy-Ohlson and G. T. Boalch, *Phycologia* **31**, 523 (1992).
13. J. M. Hayes, I. R. Kaplan, K. M. Wedeking, in *Earth's Earliest Biosphere. Its Origin and Evolution*, J. W. Schopf, Ed. (Princeton Univ. Press, Princeton, NJ, 1983), pp. 93–134.
14. N. M. Talyzina, *Rev. Palaeobot. Palynol.* **100**, 99 (1998).
15. G. A. Warburton and J. E. Zumberge, *Anal. Chem.* **55**, 123 (1983).
16. R. E. Summons and M. R. Walter, *Am. J. Sci.* **290-A**, 212 (1990).
17. J. K. Volkman, S. M. Barrett, G. A. Dunstan, S. W. Jeffrey, *Org. Geochem.* **20**, 7 (1993).
18. N. Withers, in *The Biology of Dinoflagellates*, vol. 21 of *Botanical Monographs*, F. J. R. Taylor, Ed. (Scientific Publications, Oxford, 1987), pp. 316–359.
19. J. K. Volkman, P. Kearney, S. W. Jeffrey, *Org. Geochem.* **15**, 489 (1990).
20. K. E. Peters and J. M. Moldowan, *The Biomarker Guide. Interpreting Molecular Fossils in Petroleum and Ancient Sediments* (Prentice-Hall, Englewood Cliffs, NJ, 1993).
21. L. M. Pratt, R. E. Summons, G. B. Hieshima, *Geochim. Cosmochim. Acta* **55**, 911 (1991).
22. J. M. Moldowan *et al.*, *Geology* **24**, 159 (1996); J. M. Moldowan *et al.*, in *Ecology of the Cambrian Radiation*, A. Zhuravlev and R. Riding, Eds. (Cambridge Univ. Press, Cambridge, in press).

23. This work, supported by a postgraduate fellowship, a Swedish Natural Science Research Council (NFR) grant to G. Vidal, and a NASA Planetary Biology Internship, forms part of the doctoral thesis project of N.T., which began under the supervision of the late G. Vidal. A. Johannisson provided expertise on the FACS instrument. Chemical analytical work was assisted by F. J. Fago and supported by donations to the Stanford University Molecular Organic Geochemistry Industrial Affiliates program. Reviews by P. H. Ostrom, P. Albrecht, J. Peel, and M. Moczydlowska improved the report.

28 April 1998; accepted 10 July 1998

Moho Offset Across the Northern Margin of the Tibetan Plateau

Lupei Zhu* and Donald V. Helmberger

Anomalous double-pulse teleseismic *P*-wave arrivals were observed at one station near the northern margin of the Tibetan Plateau. The azimuthal dependence of the waveform distortion and its absence at nearby stations indicated that the distortion was produced by receiver-side crustal heterogeneity. Modeling of the three-component data revealed a 15- to 20-kilometer Moho offset that occurs over a narrow lateral range of less than 5 kilometers. This east-west–striking offset separates the thick Tibetan Plateau crust from the Qaidam Basin crust. Such a sharp crustal thickness change implies a weak Tibetan Plateau crust that thickens vertically in response to penetration by India from the south and to blockage caused by a strong Qaidam Basin crust to the north.

The uplift of the Tibetan Plateau is the result of thickened crust arising from the India-Eurasia collision and the subsequent penetration of India into Eurasia. However, the mechanisms of crustal thickening are debated (*1*). Lateral heterogeneities of crustal strength are believed to play a role in determining the magnitude and distribution of deformation in a continent-continent collision (*2, 3*). The plateau has a fairly uniform elevation of about 5 km, surrounded by several low-lying sedimentary basins: the Tarim Basin to the northwest, the Qaidam Basin to the north, and the Sichuan Basin to the east (Fig. 1A). These basins are underlain by stable Precambrian cratons, which have experienced little deformation since the Paleozoic (*1, 4*). The transition of lithospheric structure from the plateau to these cratons is poorly constrained. From the analysis of teleseismic *P* waveforms, we present a model of a relatively sharp step in the Moho across the northern margin of the Tibetan Plateau.

During the 1991–1992 Sino–U.S. Tibet seismic experiment, 11 broadband stations were deployed along the Golmud-Lhasa highway (*5*) (Fig. 1A). One of the stations, TUNL, was located in the foothills of the Kunlun mountain range, which runs east and west and marks the northern boundary of the Tibetan Plateau (Fig. 1B). About 300 teleseismic events (distance range >30°) were recorded with good signal-to-noise ratios. For each event, we aligned the records of all the stations with the onsets of the *P* wave to examine the waveform variation across the array. Generally, the vertical component of the teleseismic *P* wave is less sensitive to structure near the recording site because of the wave's nearly vertical incident ray path. For this reason, the vertical component is often treated as an effective source time function of the earthquake in receiver function analyses (*6*). However, if crustal heterogeneity exists, then waveform distortion can occur. The *P* waveforms at TUNL consistently showed double-pulse arrivals from events in directions from N45°E to N70°E (Fig. 2A). Although the amplitudes of the *P* waves varied from station to station, the waveforms at most stations had a similar single-pulse shape, which is expected for the epicentral distances from a moderate earthquake at depths >40 km. However, the waveforms at TUNL consisted of two pulses separated by ~1 s. Because the similarity of waveforms at other stations ruled out the pos-

Seismological Laboratory, California Institute of Technology, Pasadena, CA 91125, USA.

*To whom correspondence should be addressed. E-mail: lupei@usc.edu. Present address: Southern California Earthquake Center, University of Southern California, Los Angeles, CA 90089, USA.